

Performance of a Carbon Fiber/Polysiloxane Composite: Thermal, Ablation, Flammability, and Mechanical Characterization

Yanan Hou¹, Colin Yee¹, Wei Li², and Joseph H. Koo^{3*}
The University of Texas at Austin, Austin, TX 78712, USA

Ben Rech⁴, Will Fahy⁵, and Hao Wu⁶
KAI, LLC, Austin, TX 78739, USA

Jarrold J. Buffy⁷
Techneglas LLC, Perrysburg, OH 3551, USA

Abstract

Fiber reinforced composite materials are widely used in the aerospace industry due to its high strength to weight ratio. One of their applications is as ablative material placed at the most outside layer of thermal protection system (TPS). TPS requires the ablative material to have low density, low thermal conductivity, high temperature resistance, formation of a stable char and high char shear strength. This paper introduces a carbon fiber (CF) reinforced polysiloxane (UHTR) composite processed and fabricated in a laboratory environment. The fabrication method of this composite is illustrated in detail. The thermal, ablation, flammability, and mechanical properties of the material are compared to a commercial ablative material, MX 4926. MX 4926 is a carbon fiber phenolic (C/Ph) composite manufactured by Solvay Cytec. In this study, the carbon fiber used to make the composite is a PAN-based 8-harness fabric provided by Hexcel. The resin, UHTR, is a colorless semi-solid polysiloxane resin manufactured by Techneglas LLC. Raw materials are firstly made into CF/UHTR prepreg sheets through a hot melt process and then molded into molding compound (MC) samples or two-dimensional (2D) laminates by a hot press. All samples for testing are post cured in a programmable oven at 350°C for 2 hours. The density of the fully cured material is measured by the water displacement method. Thermal stability, flammability, and ablation properties of the material (in the format of MC) are characterized using thermogravimetric analysis (TGA), microscale combustion calorimeter (MCC), and oxyacetylene test bed (OTB) with three different heat fluxes. Micro-structures of the ablative material before and after OTB tests are investigated and compared by the scanning electron microscopy (SEM). Mechanical properties of the material (in 2D laminates) are measured by a universal testing machine (UTM) to the ASTM standards. Testing results of the CF/UHTR material are compared with the commercial ablative material, MX 4926.

Nomenclature

CF = Carbon Fiber
CFF = Carbon Fiber Fabric

¹ Graduate Research Assistant, Texas Materials Institute, The University of Texas at Austin.

² Professor, Walker Department of Mechanical Engineering, The University of Texas at Austin.

³ Vice President & Chief Technology Officer, KAI, LLC, and Sr. Research Scientist/Research Professor, & Director, Polymer Nanocomposites Technology Lab, Walker Department of Mechanical Engineering, The University of Texas at Austin, AIAA Associate Fellow, and *corresponding author: jkoo@mail.utexas.edu.

⁴ Senior Research Engineer, KAI, LLC.

⁵ Research Engineer, KAI, LLC.

⁶ Senior Research Scientist and Business Development Manager, KAI, LLC, and AIAA Associate Member.

⁷ Product Development Manager, Techneglas LLC.

<i>CM</i>	=	Command Module
<i>C/Ph</i>	=	Carbon Fiber Phenolic
<i>HRC</i>	=	Heat Release Capacity
<i>HRR</i>	=	Heat Release Rate
<i>MC</i>	=	Molding Compound
<i>MCC</i>	=	Microscale Combustion Calorimeter
<i>OTB</i>	=	Oxy-acetylene Test Bed
POSS®	=	polyhedral oligomeric silsesquioxane
<i>SEM</i>	=	Scanning Electron Microscopy
<i>TGA</i>	=	Thermogravimetric Analysis
<i>TPS</i>	=	Thermal Protection Systems
<i>UHTR</i>	=	Ultra-High Temperature Resin
<i>UTM</i>	=	Universal Testing Machine

I. Introduction

Thermal protection system (TPS) is an important component of a reentry spacecraft. On many occasions, high temperature ablative material, placed as the most outside layer of the TPS,¹ is required to protect the components or structures of the functional parts, such as the space vehicle during the reentry stage or rocket motor nozzle. Most ablative materials are reinforced organic resin composites² due to their low densities and good ablation properties. For example, the Apollo command modules (CM) were used a low-density material, Avcoat 5026-39/HC-G, as their heat shield started in late 1960s. Avcoat 5026-39/HC-G is an epoxy-novolac resin filled fiberglass honey comb material,³ with a density of 0.51 g/cm³, a char density of about half of its virgin material density, an ablating temperature (start of pyrolysis) of 316°C, and a recession temperature (start of recession) of about 970°C.⁴ The Apollo CMs TPS were designed to tolerate a peak temperature of up to 5000°F (2760°C)¹ and experienced a peak heat flux of about 500 W/cm² with reentry times range between 800 to 900s for operational lunar missions.¹ Avcoat 5026-39/HC-G has the advantage of low density and has presented good ablative properties for medium heat fluxes, however, its manufacturing process is very time consuming and labor intensive because all the fiberglass honeycombs are required to be injected and inspected by meticulous workers. For the Mars-pathfinder project with mild heat flux (~25 W/cm²) environment in 1970s, SLA-561V was used as the heat shield material.² SLA-561V is a cork-filled and glass fiber-reinforced room-temperature curing elastomeric silicone in a phenolic honeycomb.⁵ The material was designed to tolerate a peak shear stress of 158 N/m² and the heat flux at peak shear location is about 75 W/cm². SLA-561V has presented good resistance to shear force without excessive char removal or spallation⁵ in mild heat flux conditions. For the high heat flux environments, such as Pioneer Venus in late 1970s and Galileo (Jupiter) in late 1980s, a carbon phenolic material was used for the TPS, where peak heat flux reached about 10,000 W/cm².⁶

Based on the Galileo mission, fully dense carbon phenolic is the only material that may be inherited for high heat flux environments. But the recession data from the Galileo mission also showed that the weight fraction of its TPS could not be reduced or should even be increased for a similar Jovian equatorial entry probe mission to be safer. And the weight fraction of the TPS of the Galileo was already 50%.⁶ However, there are limited researches on ablative TPS materials, especially for high heat flux environments, in the past 30 years, partially due to NASA's "risk averse" philosophy relative to TPS.⁶ For example, Koo et al. conducted a comprehensive review on the effects of nanocomposites on the performance of TPS and their ablation mechanisms, including carbon nanofibers, polyhedral oligomeric silsesquioxane (POSS®), nanosilicas and so on.⁷ Kim et al. developed a 3D printable polyetherimide nanocomposite for TPS and found its good potential for TPS application, but only for low heat flux environments.⁸

This paper introduces a carbon fiber (CF) reinforced polysiloxane composite. The material is fabricated into prepreg, laminate and molding compound for testing. Its potential of TPS applications is evaluated by comparing to a commercial ablative material, MX4926. In this study, thermogravimetric analysis (TGA) is used to evaluate the thermal stability and char yield of the material, microscale combustion calorimeter (MCC) is used to study the flammability of the material, and oxyacetylene test bed (OTB) is used to simulate the reentry conditions to investigate the performance of the material at exposure to medium to high heat fluxes. Scanning electron microscopy (SEM) is used to investigate the microstructures of the material before and after OTB tests to further study the ablative mechanism of the material. Universal testing machine (UTM) is used to measure the mechanical properties of the material.

II. Experimentation

A. Materials

The reinforcement of the composites studied in this research is a carbon fiber fabric provided by Hexcel. The fabric is made of a PAN-based carbon fiber, AS4. A polysiloxane resin was used as the matrix, provided by Techneglas LLC. Basic properties of the carbon fabric, the PAN-based carbon fiber and the polysiloxane resin are summarized in Table 1-3.

Table 1. Summary of Basic Properties of the Reinforcement in CF/UHTR

Reinforcement	Style	Weave	Count Warp	Count Fill	Warp Yarn	Fill Yarn	Area Weight, g/m ²	Thickness, mm
Carbon fiber fabrics	AGP370-8H	8-harness	22	23	AS4GP 3K	AS4GP 3K	373	0.42

Table 2. Summary of Basic Properties of the Carbon Fiber in CF/UHTR

Carbon Fiber	Tensile Strength, ksi	Tensile Modulus, msi	Strain (%)	Density, g/cm ³
AS4	638-650	33.5	1.8	1.79

Table 3. Summary of Basic Properties of the Matrix in CF/UHTR

Matrix	Appearance	Viscosity, cPs	T _g , °C	Density, g/cm ³
UHTR 6398-S	Colorless Semi-Solid	3,500 @ 70°C	>500	1.2

The material composition of the CF/UHTR are listed in Table 4 in comparison to that of the MX4926, a fully dense commercial phenolic-carbon ablative material. The density of the CF/UHTR is about 3% lower comparing to MX4926.

Table 4. Material Compositions

Material ID	Density, g/cm ³	Reinforcement, wt.%	Matrix, wt.%	Filler, wt.%	Volatile Content, wt.%
MX4926	1.47	Rayon-based carbon fiber, 41-56	SC-1008 phenolic, 31-37	Carbon black, 11-16	2-6
CF/UHTR	1.43	PAN-based carbon fiber, 57-60	UHTR 6398-S polysiloxane, 40-43	None	None

B. Fabrication of Samples

The reinforcement fabrics and semi-solid matrix are firstly combined into CF/UHTR prepreg sheets using a hot-melt procedure. CF/UHTR prepreg sheets are then cut into 0.5 inch by 0.5 inch squares to make CF/UHTR MC samples or compressed directly to make CF/UHTR 2D laminates.

1. Ideal Matrix Weight Ratio Calculation

The volume ratio of voids in the carbon fiber fabrics can be calculated by Equation 1,

$$V_{void}\% = \frac{\rho_{CF} - \rho_{CFF}}{\rho_{CF}} * 100\%, \quad \text{Equation 1}$$

where ρ_{CF} is the density of the carbon fiber, and ρ_{CFF} is the density of the carbon fiber fabrics, which can be calculated by dividing the area weight of the fabric by its thickness.

The ideal matrix weight ratio is defined as the weight ratio of the matrix when the volume ratio of the matrix equals to the volume ratio of the voids in the fabric, and can be calculated by Equation 2,

$$W_{matrix} \% = \frac{\rho_{matrix} * V_{void} \%}{\rho_{matrix} * V_{void} \% + \rho_{CF} * (1 - V_{void} \%)} * 100\%, \quad \text{Equation 2}$$

where ρ_{matrix} is the density of the matrix. Inserting values listed in Table 1-2, the ideal matrix weight ratio in this study is 40.5%.

2. Hot-Melt Prepreg Fabrication

A hot press and a programmable oven are used in the hot-melt process. Carbon fiber fabrics are cut into 12 inches by 12 inches mats for easy handling, as shown in Figure 1. The weight of each mat is measured and recorded as W_{CF} . The weight of UHTR is calculated based on the ideal matrix weight ratio. Extra 10 wt.% UHTR is added to compensate the waste loss during the process. UHTR is pre-heated at 100°C for 30 min to lower its viscosity.



Figure 1. Pre-cut carbon fiber mat (12 inches by 12 inches) laid on a hot press pre-heated at 150°C).

To make CF/UHTR prepreg sheets, a carbon fiber mat is laid on the bottom plate of a hot press that is preheated at 150°C, as shown in Figure 1. Pre-heated UHTR is spread evenly on the carbon fiber mat using a heat-resistant silicone scraper. The setup is then pressed under 5,000 psi at 150°C for 5 min, before being taken out of the hot press and cooling to room temperature on a flat surface. Top and bottom peel plies are applied for easy cleaning. The prepreg is weighted after the top and bottom peel plies peeled and excess UHTR trimmed. The weight is recorded as $W_{pre-preg}$. The real matrix weight ratio is calculated by Equation 3.

$$W_{matrix} \% = \frac{W_{pre-preg} - W_{CF}}{W_{pre-preg}} * 100\%, \quad \text{Equation 3}$$

In this study, the matrix weight ratios range from 40.2% to 43.2%.

3. Molding Compound (MC) Process

A hot press and a cylindrical mold are used in this process. Pre-made carbon fiber/UHTR prepregs are cut into 0.5 inch by 0.5 inch squares using a paper cutter, as shown in Figure 2. Pre-weighted CF/UHTR prepreg squares are placed in a 3-inch diameter three-part cylindrical mold and compressed under 2,500 psi at 150°C for 24 hours using a hot press. The temperature of the hot press is then increased to 340°C (the maximum temperature of the hot press) and soaked for 2 hours to further cure the material before demolding. To make CF/UHTR MC sample of 3 inches in diameter and 0.5 inch in thickness, as shown in Figure 3, 85 g prepreg squares are approximately needed. The CF/UHTR MC samples are post cured at 350°C for 2 hours in a programmable oven before testing.

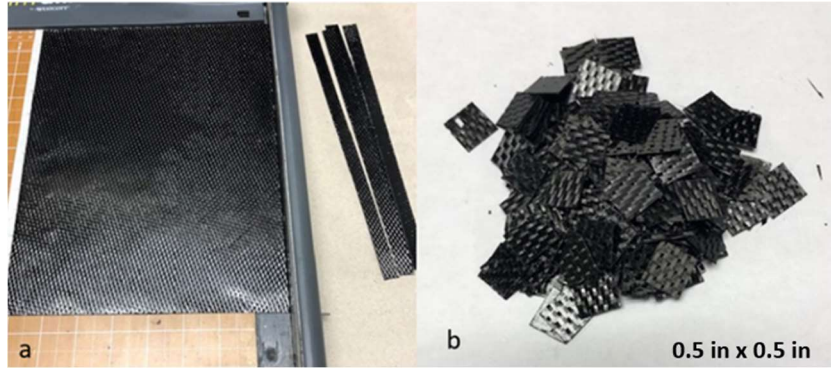


Figure 2. CF/UHTR prepregs are into a) 0.5-inch width strips; b) 0.5 inch by 0.5 inch squares.



Figure 3. A CF/UHTR MC sample (3 inches in diameter and 0.5 inch in thickness).

4. Two-Dimensional (2D) Lamination Process

A hot press is used in this process. Six layers of pre-made CF/UHTR prepregs are cut into 11 inches by 11 inches sheets, stacked up symmetrically (3 layers facing up, 3 layers facing down), and compressed under 2,500 psi at 150°C for 24 hours by a pre-heated hot press. The temperature of the hot press is then increased to 340°C for 2 hours to further cure the laminate. Top and bottom peel plies are used for easy cleaning. The laminate is post cured at 350°C for 2 hours before cutting into mechanical testing samples to ASTM standards. Figure 4 shows a CF/UHTR 2D laminate sample.



Figure 4. A CF/UHTR 2D laminate sample (11 inches by 11 inches by 0.1 inches).

C. Materials Characterization

1. Thermogravimetric Analysis (TGA)

A thermogravimetric Analyzer (TGA/DSC 1 STAR[®] System by Mettler Toledo), as shown in Figure 5, is used to compare the thermal stability and char yields of the MX4926 and CF/UHTR composites. TGA measures weight losses of testing materials as temperature increasing. In TGA tests, both materials (~15 mg) are dried at 150°C isothermally for 30 minutes and directly heated up to 1,000°C at 20°C/min in both air and nitrogen environments.



Figure 5. Thermogravimetric Analyzer (TGA/DSC 1 S STAR[®] System) by Mettler Toledo.

Char yield of the material is defined as the residue weight of the material at 1,000°C divided by its weight after the isothermal drying period tested in nitrogen with a heating rate of 20°C/min.

2. Microscale Combustion Calorimetry (MCC)

A Microscale Combustion Calorimeter (MCC2, Govmark, Inc.), as shown in Figure 6, is used to study thermal combustion properties of the materials according to ASTM D7309-2007. MCC measures heat release rates of a material as temperature increases. In MCC tests, both materials (2-3 mg) are heated up rapidly from 100°C to 700°C at 1°C/s in the environment of 80 mL/min nitrogen and 20 mL/min oxygen. Heat release rate and heating rates are recorded as temperatures. From MCC results, the heat release capacity (HRC), peak heat release rate (HRR), and the temperature of peak HRR of the material can be obtained. At least three repeated samples of each material are tested to calculate error bars.



Figure 6. Microscale Combustion Calorimeter (MCC-2) by Govmark Organization Inc.

3. Oxyacetylene Test Bed (OTB)

The OTB test is used to study the ablation properties of the materials. CF/UHTR MC and MX4926N MC (material ID of MX4926 in the format of molding compound) samples are cut into cylindrical OTB samples of 30 mm (1.18 inches) in diameter and half inch in thickness by a waterjet. The OTB sample is mounted in a crucible with an ID that is slightly larger than the diameter of the OTB sample with a silicone rubber. The top surface of the OTB sample is leveled with the top of the crucible. The depth of the crucible is larger than the thickness of the OTB sample. A wire K-type thermocouple is inserted through a 2 mm diameter hole at the bottom of the crucible and contacted the backside of the OTB sample. During the OTB test, the crucible is clamped on a chunk holder. A torch with a #4 victor welding tip approaches the top surface of the OTB sample to simulate reentry conditions. A 4:3 oxygen and acetylene ratio are used as the fuel supply. Figure 7 shows a sketch of the OTB setup.

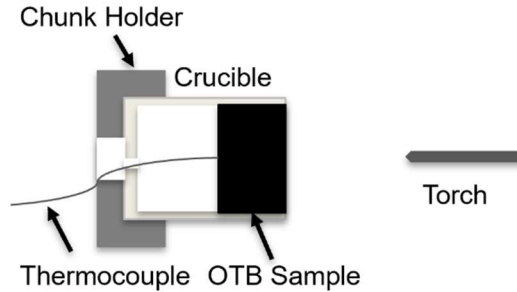


Figure 7. Sketch of the OTB setup.

Three conditions are simulated, as listed in Table 5. Various heat fluxes are obtained by adjusting the standoff distance between the torch and the top surface of the OTB sample and calibrated by a Vatell Gardon heat flux transducer (Thermogage 1000-54).

Table 5. Simulated Reentry Conditions

Condition		Ablation Parameter, kJ/cm ²
Heat Flux, W/cm ²	Exposure Time, s	(i.e., heat flux X exposure time)
500	60	30
1,000	60	60
1,500	60	90

Heights (or thicknesses) and masses of OTB samples are measured before and after OTB tests. After-testing heights are taken at the lowest point of the samples. Backside temperatures during the OTB tests are measured by the thermocouple shown in Figure 7. Top surface temperatures are measured by a pyrometer. OTB results are presented as recession percentages (Equation 4), mass losses (Equation 5), surface and backside temperatures versus ablation parameters.

$$\text{Recession Percentage} = \frac{\text{Initial Height} - \text{Final Height}}{\text{Initial Height}} * 100\%, \quad \text{Equation 4}$$

$$\text{Mass Loss} = \frac{\text{Initial Weight} - \text{Final Weight}}{\text{Initial Weight}} * 100\%, \quad \text{Equation 5}$$

4. Scanning Electron Microscopy (SEM)

A SEM (FEI Quanta 650 ESEM) is used to investigate microstructure changes of the material before and after OTB tests. Samples are coated with gold by an EMS putter coater. A voltage of 20 kV is used for the tests.

5. Mechanical Test

A Shimazu universal testing machine is used to evaluate the mechanical properties of the material, as shown in Figure 8.



Figure 8. Shimadzu Universal Testing Machine: Tensile testing set-up.

Tensile properties of CF/UHTR 2D laminate samples are tested to ASTM D3039. Five samples are used for the test. Strain gauges (CEA-09-250UT-350) by Micro-Measurements are attached in the middle of each tensile bar to measure the strain during the tests, as shown in Figure 9.

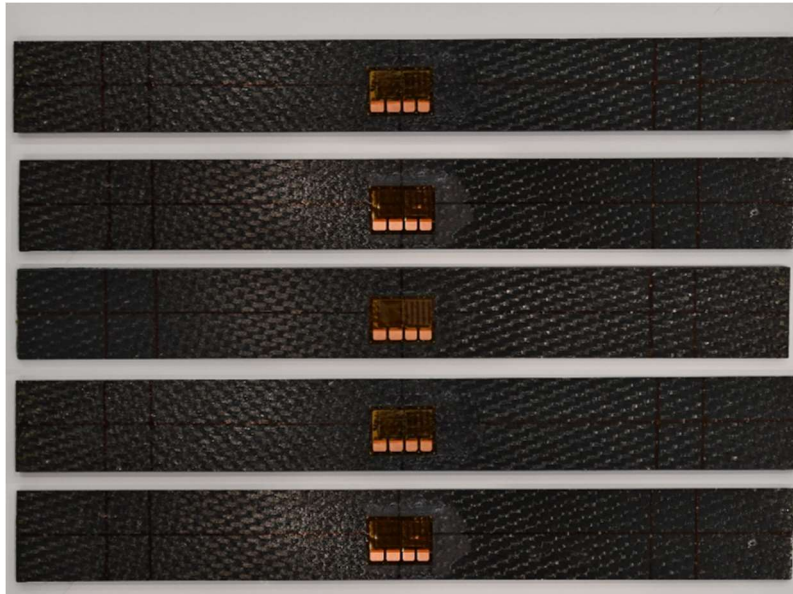


Figure 9. Tensile testing sample with strain gauge.

III. Results and Discussion

A. TGA results

Figure 10 shows weight changes of CF/UHTR MC and MX4926N MC samples at elevated temperatures in nitrogen and air. In both tests in air and nitrogen, MX4926N MC samples (green dash dotted line and blue dash line) have lost about 2% weights during the isothermal drying periods (150°C for 30 min). This is due to the phenolic matrix in MX4926N MC, which is known for moisture taken. The TGA results show that MX4926N MC (green dash dotted line) decomposes after 200°C, followed by a quick decomposition at around 400°C and a quicker decomposition at

around 520°C. CF/UHTR MC (red solid line) is stable up to 400°C followed by one quick single step decomposition process. Char yield is defined as the weight of the material at 1,000°C divided by its weight after the isothermal period in nitrogen environment. The heating rate is set at 20°C/min. As listed in Table 6, the char yield of MX4926N MC is calculated to be 84%, which is very high. The char yield of CF/UHTR MC at the same condition is even higher, yields 93%. In air, both materials show similar trends to their performances in nitrogen at temperatures below 600°C. At elevated temperatures, both materials are further decomposed due to oxidative reactions in the presence of oxygen. CF/UHTR MC (orange dotted line) has a residue weight of 25 wt.% at 920°C and stabilized to the end of the test, whereas MX4926N MC (blue dash line) is completely decomposed at 880°C.

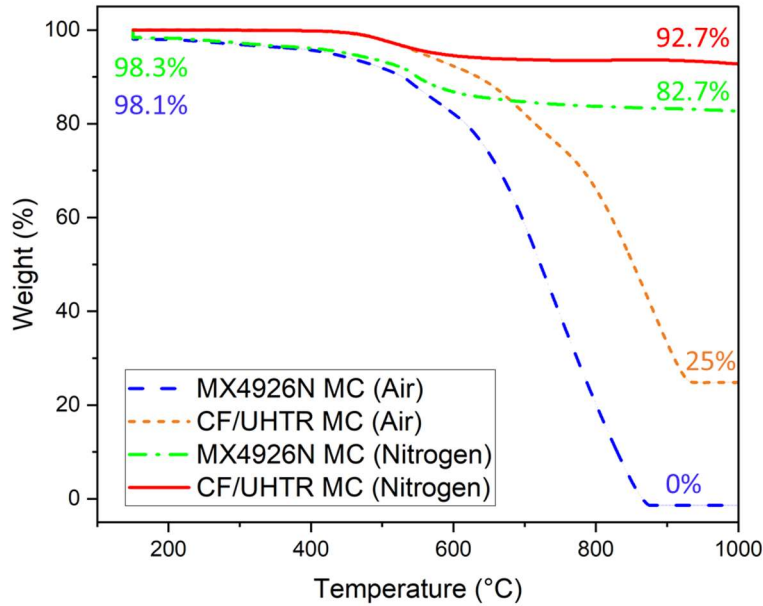


Figure 10. TGA mass loss curves (TGA, heating rate of 20°C/min in air and N₂).

Table 6. Char Yield Comparison of CF/UHTR MC and MX4926N MC

Material ID	CF/UHTR MC	MX4926N MC
Char Yield, %	92.7	84.1

B. MCC results

Figure 11 shows representative heat release rate curves of the CF/UHTR MC and MX4926N MC materials over temperatures. MX4926 is known for its good flammability properties. The peak HRR of MX4926N MC is 46.6 W/g, while that of the CF/UHTR MC is 25.6 W/g, which is even 45% lower comparing to MX4926N MC. Three samples of each material are tested, all results are summarized in Figure 12. CF/UHTR MC presents a significantly smaller peak HRR and HRC. In addition, the temperature of the peak HRR of CF/UHTR MC is lower than that of the MX4926N MC material.

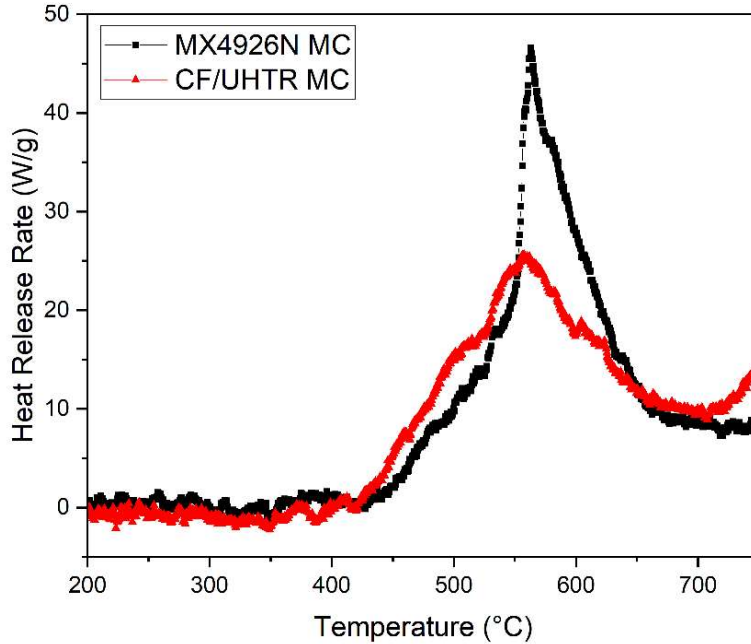


Figure 11. Representative HRR curves (MCC, heating rate of 1°C/s in 20% O₂ and 80% N₂).

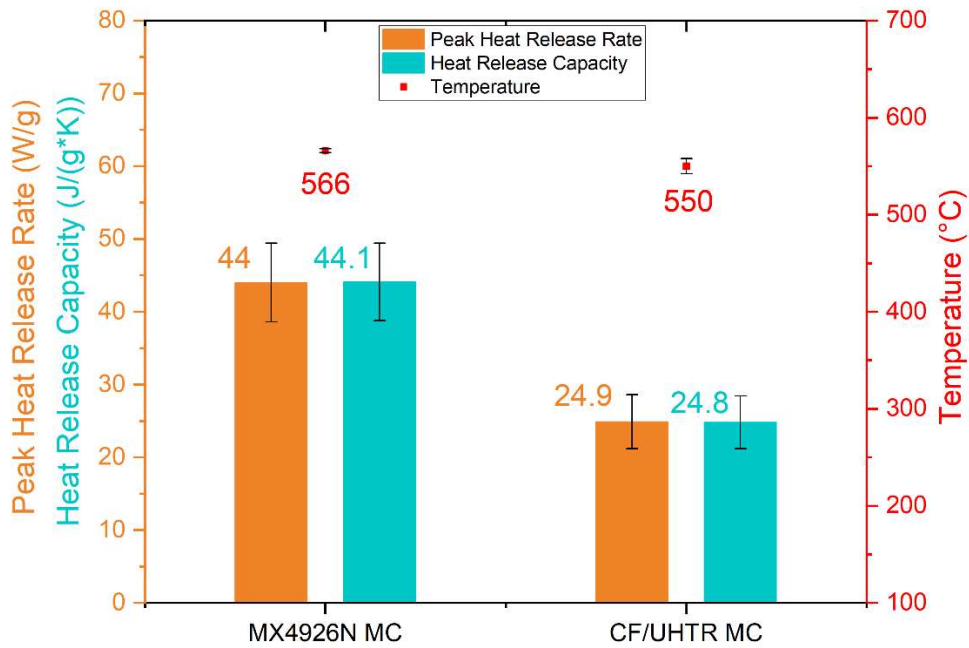


Figure 12 Summary of MCC results of CF/UHTR MC and MX4926N MC materials.

C. OTB results

Figure 13 shows recession percentages of the CF/UHTR MC and MX4926N MC materials over ablation parameters. Ablation parameter is defined as the heat flux multiplies the time that the material exposed to the OTB flame. Both materials present negative recession percentages at all tested conditions, which implies the materials have swelled more than receded during the OTB tests. To separate the swell and material loss, the mass losses of both materials are plotted as ablation parameters, as shown in Figure 14.

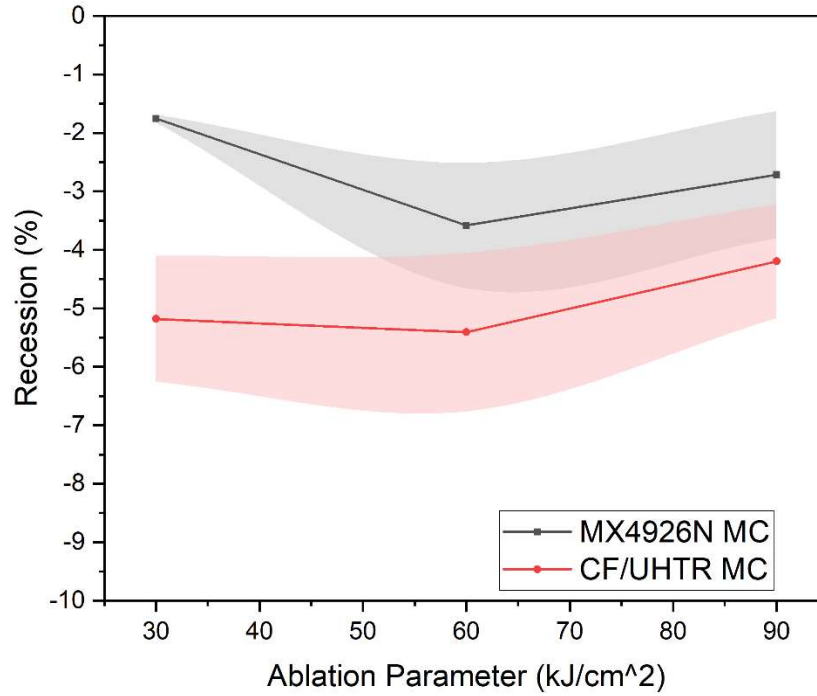


Figure13. Summary of recession percentage results in OTB tests.

Figure 14 shows that the mass losses of both materials increase as the ablation parameter increases. Mass losses of the CF/UHTR MC are approximately 1/8 of those of the MX4926N MC material in all test conditions, which shows that CF/UHTR MC has better ablation property.

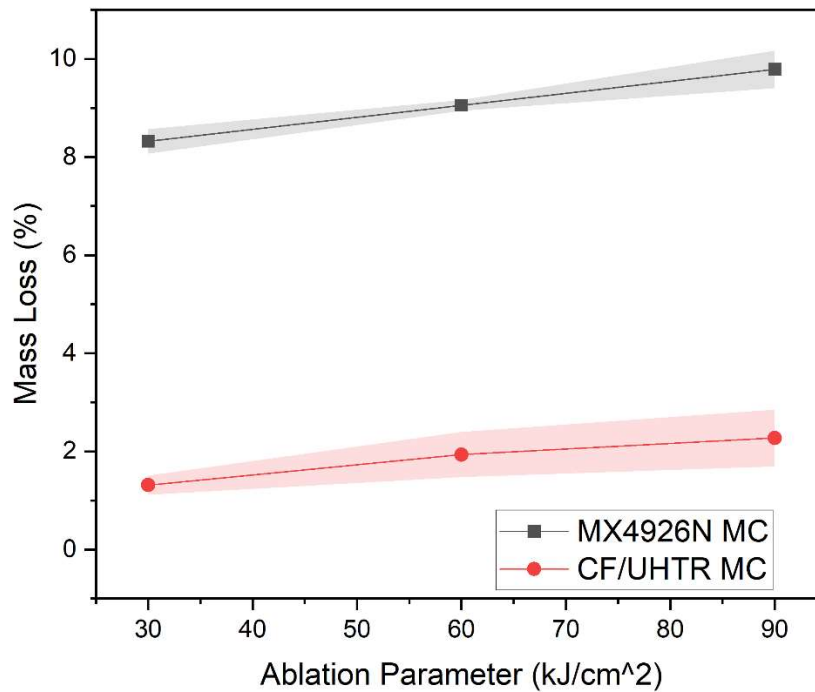


Figure 14. Summary of mass loss results in OTB tests.

Figure 15 shows the top surface temperatures and the backside temperatures of CF/UHTR MC and MX4926N MC in the OTB tests. Temperatures of both materials are similar in all testing conditions. Surface temperatures of both materials have reached above 1,800°C, the backside temperatures of both materials are remained around 250°C. These results indicate that both materials have very good thermal insulation property.

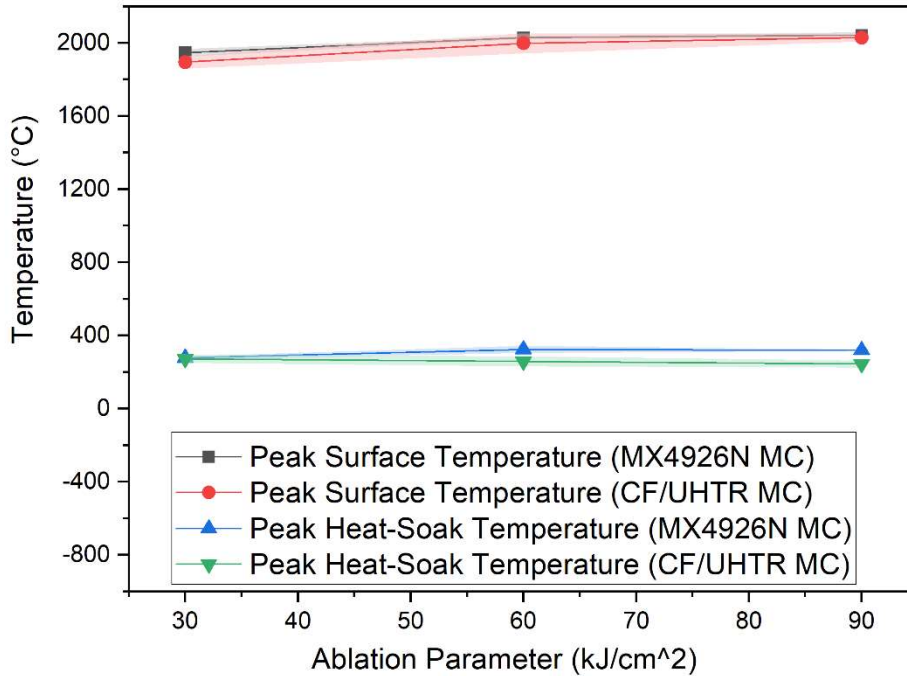


Figure 15. Summary of temperature results in OTB tests.

CF/UHTR MC OTB samples before and after OTB tests are embedded in low temperature curing clear epoxy and cut by a tile saw to investigate their cross-sections. The clear epoxy helps to keep the integrity of the charred OTB samples, especially the ones after OTB tests. Figure 16 shows the middle 1/5 of cross-sections of CF/UHTR MC OTB samples before and after OTB tests. O represents the center of the bottom of the OTB samples, Z-axis is in the thickness direction and r-axis is in the radial direction. Cross sections of the samples after OTB tests do not show obvious char, pyrolysis and virgin zones like traditional ablative materials,² but show clearly that the amount of voids increases through the thickness direction as the ablation parameter increases.

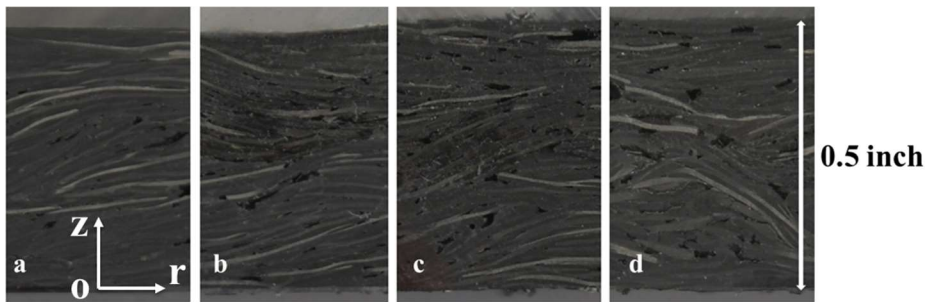


Figure 16. Cross-section of CF/UHTR OTB samples: a) before OTB test; b) AP=30 (kJ/cm²); c) AP=60 (kJ/cm²); and d) AP=90 (kJ/cm²).

D. SEM analysis

Figure 17 compares SEM images of CF/UHTR MC before and after the OTB test with the ablation parameter of 90 kJ/cm². It shows that after the OTB test, the binding matrix, UHTR, has de-bonded compressed carbon fibers and the fiber relaxation results in material swelling and voids inside of the material. The material is expected to eventually

recede at higher heat flux or longer exposure time, but it added a swelling and permeability increasing step on the top of the traditional ablation mechanism.

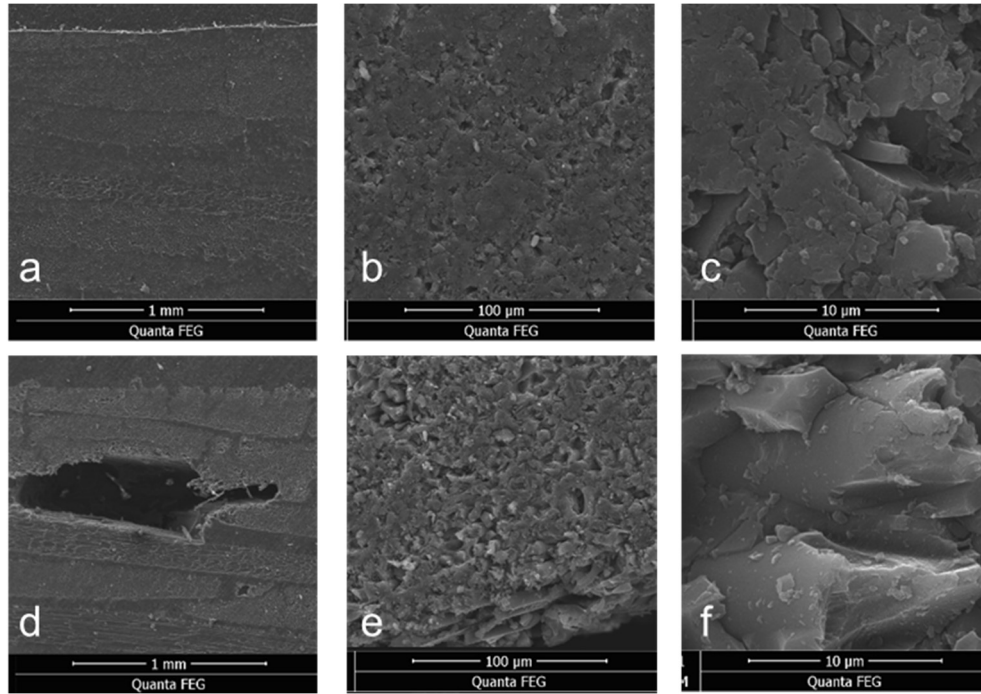


Figure 17. SEM images of CF/UHTR MC before (a, b, and c) and after the OTB test: AP=90 kJ/cm² (d, e, and f).

E. Mechanical test results

Figure 18 shows a representative stress and strain curve of CF/UHTR 2D laminate sample. The fracture is marked by “x”. The maximum stress is defined as the ultimate tensile strength. The slope of the linear zone defines the Young’s Modulus. Five tests are conducted to calculate the error bars, results are summarized in Figure 19.

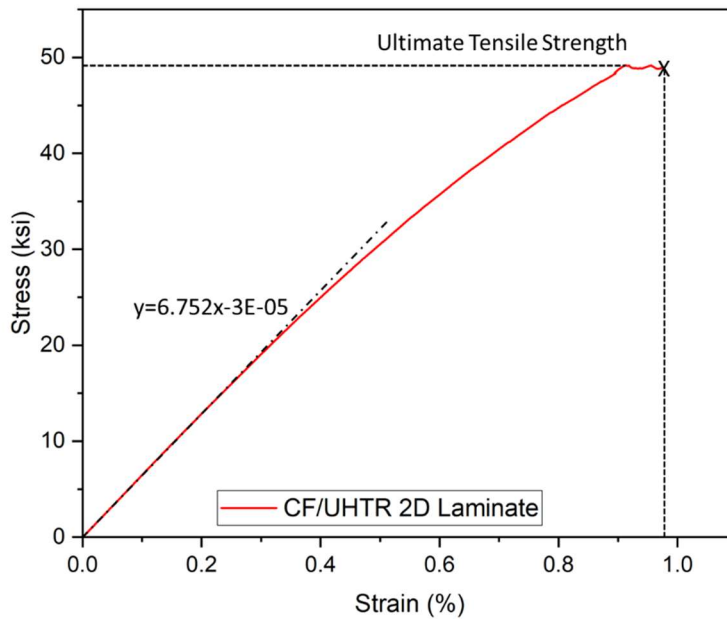


Figure 18. Representative stress and strain curve of CF/UHTR 2D laminate material.

Figure 19 shows that CF/UHTR laminates have a tensile strength of 49.6 ksi, which is 2.4 times of the tensile strength of MX4926 laminates. The Young's Modulus of the CF/UHTR laminates is 6.6 msi, which is 2.64 times of that of MX4926 laminates. Elongations of both materials tend to be low, which are 0.97% for CF/UHTR laminates and 1.2% for MX4926 laminates.

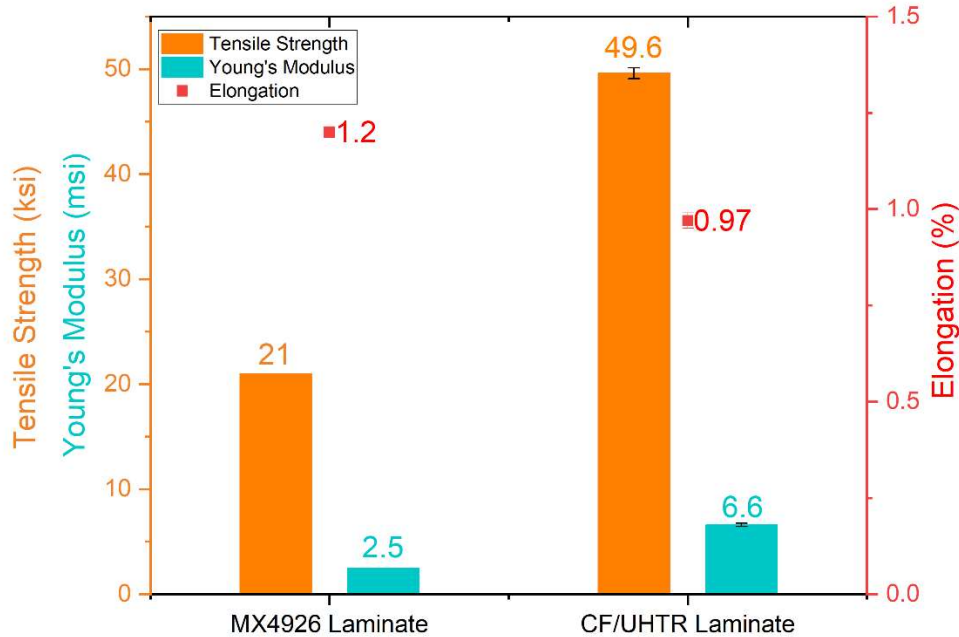


Figure 19. Summary of tensile properties.

IV. Conclusions

In this study, a CF/UHTR composite is introduced and its potential for TPS applications is evaluated. Comparing to the commercial ablative material, MX4926, advantages of the CF/UHTR material are summarized as follow:

- Lower density (approximately 3% lower).
- Higher decomposition temperature and higher char yield (10% higher).
- Lower peak heat release rate at lower temperature and smaller heat release capacity (43% lower).
- Less mass loss at exposure to high heat fluxes (88% less).
- Comparable thermal insulation.
- Higher tensile strength (1.4 times higher) and higher Young's Modulus (1.64 times higher).

Acknowledgments

This research is partially funded by Techneglas LLC, Perrysburg, OH, USA. The authors acknowledge the use of facilities and the technical assistance of the Advanced Composites International, LLC, Round Rock, TX, USA. The authors appreciate Dr. Abiodun Oluwalowo from Florida State University for conducting the thermal conductivity measurement. The authors acknowledge Hexcel for providing carbon fiber fabrics.

References

1. Pavlosky, J. E. & St Leger, L. G. Apollo experience report: Thermal protection subsystem. *Apollo Int. Mag. Art Antiq.* (1974).
2. Laub, B. & Venkatapathy, E. Laub, Venkatapathy - 2003 - Thermal Protection System Technology

- and Facility Needs for Demanding Future Planetary Missions. **544**, 239–247 (2004).
3. Bartlett, E. P., Anderson, L. W. & Curry, D. M. An evaluation of ablation mechanisms for the apollo heat shield material. *J. Spacecr. Rockets* **8**, 463–469 (1971).
 4. Williams, S. D. & Curry, D. M. Thermal protection materials: Thermophysical property data. 236 (1992).
 5. Tauber, M. *et al.* Tests of SLA-561V Heat Shield Material for Mars-Pathfinder. *Nasa-Tm-110402* (1996).
 6. Edquist, K. T. *et al.* Mars science laboratory entry capsule aerothermodynamics and thermal protection system. *IEEE Aerosp. Conf. Proc.* (2007) doi:10.1109/AERO.2007.352823.
 7. Koo, J., Natali, M., Tate, J. & Allcorn, E. Polymer nanocomposites as ablative materials: A comprehensive review. *Int. J. Energ. Mater. Chem. Propuls.* **12**, 119–162 (2013).
 8. Kim, S. *et al.* Development of polyetherimide composites for use as 3D printed thermal protection material. *J. Mater. Sci.* **55**, 9396–9413 (2020).